

# ZnO Nanotubes Grown at Low Temperature Using Ga as Catalysts and Their Enhanced Photocatalytic Activities

Joonho Bae,<sup>†</sup> Jing Bin Han,<sup>‡</sup> Xiao-Mei Zhang,<sup>†,§</sup> Min Wei,<sup>†,‡</sup> Xue Duan,<sup>‡</sup> Yue Zhang,<sup>§</sup> and Zhong Lin Wang<sup>\*,†</sup>

School of Materials Science and Engineering, Georgia Institute of Technology, Atlanta, Georgia 30332, State Key Laboratory of Chemical Resource Engineering, Beijing University of Chemical Technology, Beijing 100029, P. R. China, and Department of Materials Physics and Chemistry, University of Science and Technology Beijing, Beijing 100083, P. R. China

Received: September 11, 2008; Revised Manuscript Received: April 8, 2009

We report the synthesis of ZnO nanotubes grown via the Ga-catalyzed vapor transport method at low temperature and their photocatalytic activity. The low melting point of Ga (29 °C) resulted in the growth of ZnO nanotubes at a low temperature of 80 °C, enabling us to use Kapton film or ITO glass as substrates. Structure analysis shows that the nanotube is single crystal and has a hollow structure with a wall thickness of ~2 nm, is several tens of micrometers long, and has a diameter of 60–300 nm. Photocatalytic activity of ZnO nanotubes was determined by measuring the photoinduced degradation of rhodamine B (RB) and an azobenzene-containing polymer poly{1-4[4-(3-carboxy-4-hydroxyphenyl-azo)benzenesulfonamido]-1,2-ethanediyl sodium salt} (PAZO) solution, respectively. The measurement reveals that the photodecomposition reactions of both RB and PAZO follow the first-order rate law with the rate constant of 0.018 and 0.004 s<sup>-1</sup>, respectively. The photocatalytic activity of ZnO nanotubes was shown to be much enhanced compared with ZnO thin films and ZnO nanowires. Therefore, this work demonstrates a novel and simple way to synthesize ZnO nanotubes on flexible substrates, which can potentially serve as excellent photocatalysts for the degradation of organic pollutants in water.

In the past few years, ZnO, one of the oxide semiconductors, has attracted considerable interest due to its unique material properties such as direct and wide bandgap (3.2 eV), *n*-type semiconducting properties, large binding energy (60 meV at room temperature), and piezoelectricity.<sup>1–3</sup> In addition, the photocatalytic activity of ZnO has also been studied owing to its high photocatalytic efficiency. It is known that ZnO can degrade most kinds of organic compounds, dyes, and detergents under UV-irradiation.<sup>4</sup> However, previous studies have paid attention to thin films or fine powders of ZnO as photocatalysts, and reports on photocatalytic properties of ZnO nanostructures are rarely performed.<sup>5,6</sup> Among various nanostructures, one-dimensional ZnO nanostructures such as nanowires<sup>7</sup> and nanoneedles<sup>5</sup> were shown to be good photocatalysts due to their high surface-to-volume ratio.

For applications as photocatalysts, tubular structure could provide larger specific surface-to-volume area than nanowires or nanoneedles because of their hollow internal structure, resulting in the enhancement of photocatalytic activity. Besides the application of nanotubes for photocatalysts, tubular nanostructures of various materials have attracted intensive interest since they could be used as nanoscale building blocks with unique physical properties.<sup>8–10</sup> As stimulated by the research in carbon nanotubes,<sup>11</sup> there have been substantial reports on tubular nanostructures of various materials including GaN,<sup>12</sup> MoS<sub>2</sub>,<sup>13</sup> TiO<sub>2</sub>,<sup>14</sup> SiO<sub>2</sub>,<sup>15</sup> Al<sub>2</sub>O<sub>3</sub>,<sup>16</sup> and ZnO.<sup>1,17–20</sup> ZnO nanotubes have been synthesized using high-temperature (700 °C) vapor

phase growth,<sup>17</sup> first reduction, and following oxidation of ZnS powders,<sup>18</sup> thermal treatment of [Zn(NH<sub>3</sub>)<sub>4</sub>]<sup>2+</sup> precursor in ethanol solvent,<sup>19</sup> pyrolysis of zinc acetylacetonate,<sup>20</sup> and hydrothermal growth.<sup>1</sup>

In this article, we report on the fabrication of ZnO nanotubes at relatively low temperature (80 °C) using Ga as catalyst on ITO glass or Kapton film substrates. Their crystal structure was characterized, and the photocatalytic performance was studied for the degradation of dyes. To the best of our knowledge, this work is the first investigation on photocatalytic behavior of tubular ZnO nanostructures grown at low temperature using ITO glass or Kapton film substrates. The ZnO nanotubes in this work have been demonstrated to work as effective photocatalysts by virtue of their high surface-to-volume ratio and low band gap.

**Synthesis of ZnO Nanotubes.** To synthesize ZnO nanotubes, Ga catalyst was thermally deposited on ITO glass or Kapton films with a thickness of ~20 nm. Zn powder (Sigma-Aldrich, 99.99%) was used as the vapor source of ZnO. The substrate and Zn powder were mounted in a tube furnace with two temperature zones. Zn powder (melting point of 420 °C) was placed in the high temperature zone of the furnace. The entire growth system was evacuated to <5 mTorr, and the high temperature zone was heated up to 850 °C to evaporate the source materials. The substrate was placed in the same tube in the lower temperature zone of 80 °C. Once the temperatures of 850 and 80 °C were achieved, a mixture of Ar and O<sub>2</sub> gas was introduced to the tube furnace at the rates of 120 and 8 sccm (standard cubic centimeters per minute), respectively, to grow ZnO nanotubes on the substrate. The low melting point of Ga (29 °C) resulted in the formation of molten Ga droplets to provide seeds to grow nanotubes at a low temperature of 80 °C. A total pressure of ~3 Torr was maintained throughout the

\* Corresponding author. E-mail: zhong.wang@mse.gatech.edu.

<sup>†</sup> Georgia Institute of Technology.

<sup>‡</sup> Beijing University of Chemical Technology.

<sup>§</sup> University of Science and Technology Beijing.

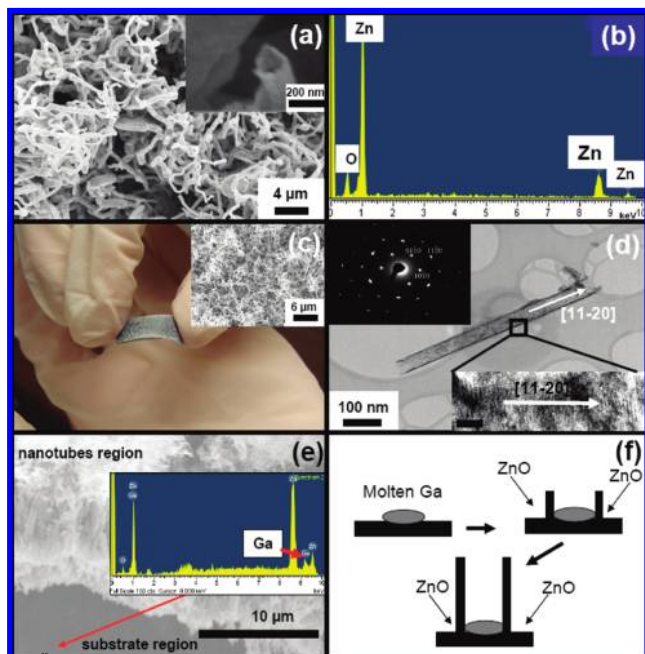


**Figure 1.** (a) SEM image of as-grown ZnO nanotubes on an ITO glass substrate. The inset shows an open end of the nanotube. (b) EDS result of single ZnO nanotube showing Zn and oxygen content. (c) A picture of as-grown ZnO nanotubes on a Kapton film. Low temperature growth enables a flexible substrate for ZnO nanotubes. The inset exhibits the SEM image of ZnO nanotubes. (d) TEM image of a ZnO nanotube which shows that both ends are open and the inside structure is hollow. The upper inset displays diffraction pattern of the nanotube, indicating its single-crystal structure. The lower inset is a high-resolution TEM image of the nanotube. The scale bar in the lower inset: 10 nm. (e) SEM and EDS reveal that Ga remains at the bottom of the nanotubes. When an electron beam was shined on a substrate region where initial ZnO nanotubes are removed, Ga content was found in the EDS spectrum. (f) Proposed growth mechanism of ZnO nanotubes.

growth of ZnO nanotubes. After 10 min of reaction, the furnace was cooled to room temperature without gas flow.

#### Electron Microscopy Characterization of ZnO Nanotubes.

The morphology of the as-grown ZnO nanotubes was examined by an FEG scanning electron microscope LEO 1530 SEM. Transmission electron microscopy was performed on ZnO nanotubes using JEOL 4000 EX. For TEM, nanotubes were transferred to a copper TEM grid by mechanically detaching nanotubes from the substrates. Energy dispersive spectroscopy was performed by EDS attached to the SEM and TEM. Figure 1 shows SEM images of as-grown ZnO nanotubes on an ITO glass (Figure 1a) and a Kapton film (Figure 1c). As can be seen in the figures, large amount of nanowire-like structures were observed over the large area of the substrate (more than 1 cm<sup>2</sup>). The inset in Figure 1a displays an open end of the nanowire-like structures, suggesting hollow character. The tubular structure is further confirmed by TEM (Figure 1d). The diameter of typical nanotubes ranges from 60 to 300 nm. Their length is estimated to be approximately several tens of micrometers. To characterize chemical composition of nanotubes, an electron dispersive spectroscopy attached to the scanning electron microscope was utilized. EDS measurement of the nanotubes reveals that they are composed of Zn and O with a molar ratio of close to 1:1, indicating the formation of ZnO nanotubes (Figure 1b).

Gallium was used in this work as a catalyst to synthesize the nanotubes. Since Ga has a low melting point of 29 °C, it forms a liquid droplet at even considerably low growth

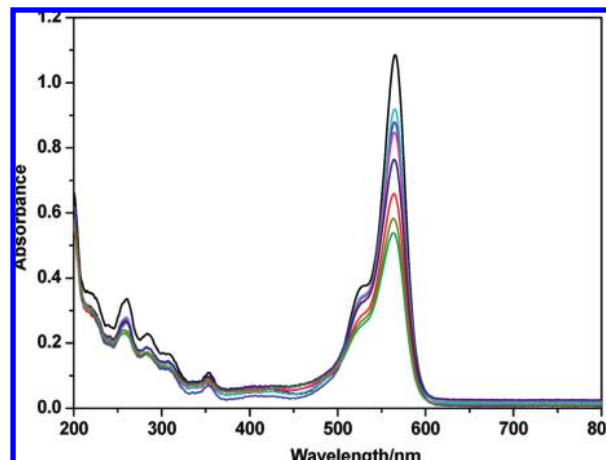


**Figure 2.** UV-vis absorption spectra of RB as a function of irradiation time with the absence of ZnO nanotubes. The time interval between two curves is 20 min from top to bottom. The initial solution concentration was purposely chosen to give an absorbance value above 1.0.

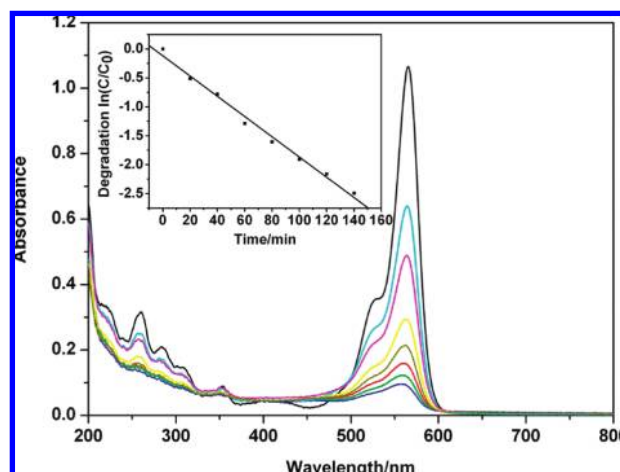


**Figure 3.** UV-vis absorption spectra of RB as a function of irradiation time with the presence of ZnO nanotubes. The time interval between two curves is 20 min from top to bottom. The initial solution concentration,  $C_0$ , was purposely chosen to give an absorbance value above 1.0.  $C$  is the concentration of the remaining molecules at the given time. Inset shows the plot of degradation  $\ln(C/C_0)$  as a function of irradiation time. The linearity of this plot indicates the photodegradation of RB with ZnO nanotubes follows the first-order rate law with the reaction constant of 0.018 s<sup>-1</sup>.

temperature of 80 °C. Generally, the high temperature vapor phase growth method (more than 700 °C) was carried out in previously reported work, making it difficult to make use of flexible substrates. Our approach of using Ga as catalyst facilitates the application of flexible substrates such as Kapton films. Figure 1c shows as-grown ZnO nanotubes on a Kapton film.

Figure 1d shows TEM images of a ZnO nanotube with the diameter of 60 nm. It can be seen clearly that both ends of the nanotube are open, and the hollow internal structure possesses a wall thickness of ~2 nm, confirming the tubular morphology. The diffraction pattern from the nanotube demonstrates its single-crystal structure.

To understand the growth mechanism of ZnO nanotubes, some nanotubes are removed from the substrate, and the electron beam is shined on the exposed area of the substrate. EDS measurement on the area reveals that Ga content remains at the bottom of ZnO nanotubes (Figure 1e). In Figure 1e,

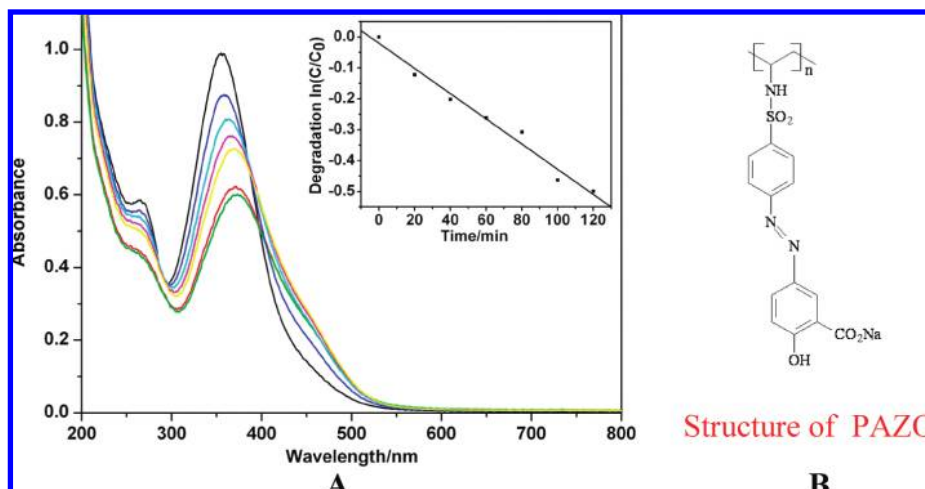


**Figure 4.** (A) UV-vis absorption spectra of PAZO as a function of irradiation time with the presence of ZnO nanotubes. The time interval between two curves is 20 min from top to bottom. The initial solution concentration was purposely chosen to give an absorbance value above 1.0. Inset shows the plot of degradation  $\ln(C/C_0)$  as a function of irradiation time. The linearity of this plot indicates the photodegradation of PAZO with ZnO nanotubes follows the first-order rate law with the reaction constant of  $0.004 \text{ s}^{-1}$ . (B) The molecular structure of PAZO.

still Zn and O peak are seen in the EDS spectrum since ZnO was not completely cleaned from the ITO substrate. ZnO was removed by mechanical scratch, leaving some ZnO contents on the substrate. Extensive EDS and TEM measurements on as-grown individual nanotubes did not show Ga catalysts at the top of nanotubes. Hence, the Ga catalyst is thought to be located at the root of the nanotubes after the growth process is finished.

On the basis of the above observations from SEM, TEM, and EDS measurements, the active growth surface is thought to be at the root of the nanotube, and the growth of nanotubes occurs by vapor-liquid-solid (VLS) process (Figure 1f). Since Ga has a very low melting point ( $29 \text{ }^\circ\text{C}$ ), it forms molten droplets on the substrate. The surface of liquid Ga supersaturates by constant supply of ZnO vapor. Thus, the ZnO nanotubes continue to grow by using molten Ga droplets as nucleation seeds. The growth mechanism of carbon nanotubes may provide some insights to understand how ZnO nanotubes are formed. More studies would be needed to understand the formation mechanism of ZnO nanotubes.

**Measurement of Photocatalytic Activity of ZnO Nanotubes.** To evaluate the photocatalytic activity of the synthesized ZnO nanotubes on Kapton films, two kinds of dyes, rhodamine B (RB) and an azobenzene-containing polymer poly{1-4[4-(3-carboxy-4-hydroxyphenyl-azo)benzenesulfonamido]-1,2-ethanediyl sodium salt} (PAZO), were chosen as model molecules for the photodegradation investigation. A sample of 3 mL of  $1 \times 10^{-5} \text{ M}$  RB or  $6.75 \times 10^{-5} \text{ M}$  PAZO solution was added into a typical quartz cell, and a substrate with the ZnO nanotubes with a size of  $1.1 \text{ cm} \times 0.8 \text{ cm}$  was vertically immersed into the solution. The quartz cell was irradiated by UV-light produced with a 500 W mercury lamp. The cell was placed about 15 cm from the light source to minimize the heat effect. The UV-vis absorption spectra of the solution as a function of irradiation time were recorded by using a Shimadzu UV-2501PC spectrophotometer after removing the substrate. The substrate was placed back into the solution for further irradiation at intervals of 20 min for up to 140 min. Moreover, the self-degradations of both RB and PAZO were also studied, by using the dye solution as a reference sample in the absence of ZnO nanotubes under the same irradiation conditions. The decomposed contents of dye were calculated by  $100(1 - I/I_0)$ , where  $I$  and  $I_0$  are the

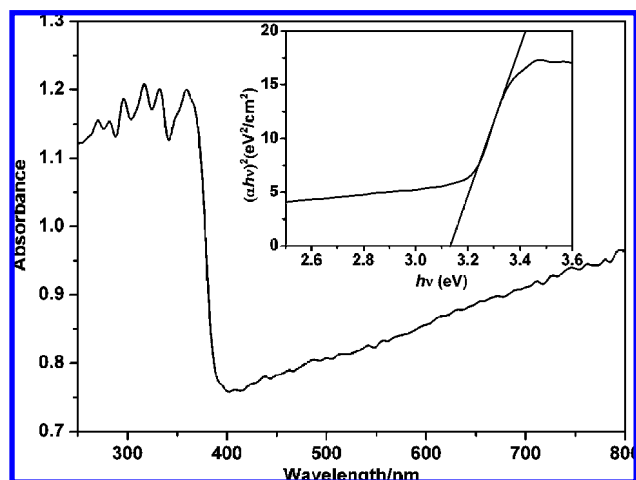


**Figure 5.** UV-vis diffuse reflectance spectrum of the as-synthesized ZnO nanotubes on an ITO glass substrate. The inset displays a plot of  $(\alpha h\nu)^2$  vs  $h\nu$  for the determination of the direct band gap of the nanotubes ( $3.13 \text{ eV}$ ).

absorbance band intensity of the sample and the control, respectively.<sup>5</sup>

It was found that the molecule of RB degrades itself under irradiation of UV in the absence of ZnO nanotubes (Figure 2). However, the presence of the ZnO nanotube catalyst increases its degradation process significantly. Figure 3 shows the changes in the UV-vis absorption spectra of RB over 140 min, indicating the nanotube material is an effective photocatalyst. After 140 min, the fraction of the decomposed dye was  $\sim 92\%$ . The degradation ratio with respect to time is also given (inset of Figure 3). This plot of  $\ln(C/C_0)$  vs time is linear, indicating that the photodecomposition reaction follows the first-order rate law. The rate constant was calculated to be  $0.018 \text{ s}^{-1}$  from the slope of the curve. In the case of PAZO, no obvious self-degradation was observed without ZnO nanotubes under irradiation of UV (not shown). However, the existence of ZnO nanotubes favors the occurrence of this reaction. Figure 4 displays the changes in the UV-vis absorption spectra of PAZO over 120 min in the presence of ZnO nanotubes. The linear relationship between  $\ln(C/C_0)$  and irradiation time indicates that the photodegradation process of PAZO can be described by the first-order

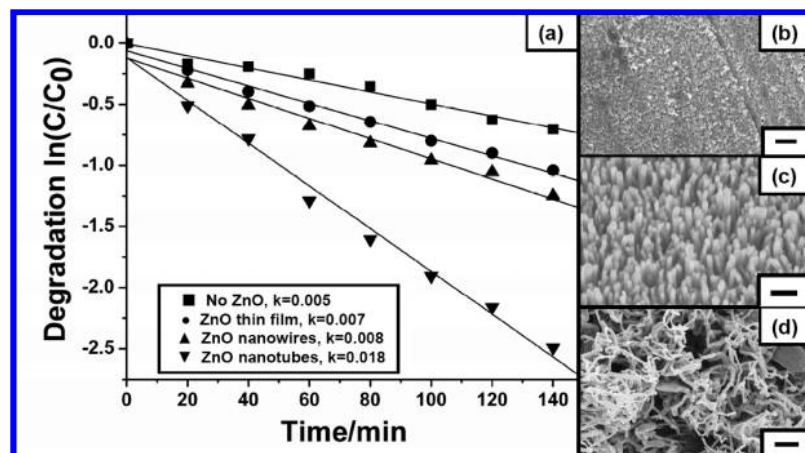


**Figure 6.** (a) Plot of degradation  $\ln(C/C_0)$  as a function of irradiation time by RB without any photocatalysts (■), ZnO thin film (●), ZnO nanowires (▲), and ZnO nanotubes (▼). The test dye was RB. The reaction constants for each experimental conditions were shown in the inset. (b) SEM image of ZnO thin film. The scale bar:  $3 \mu\text{m}$ . (c) SEM image of ZnO nanowires. The scale bar:  $400 \text{ nm}$ . (d) SEM image of ZnO nanotubes. The scale bar:  $4 \mu\text{m}$ .

rate law. The rate constant was calculated to be  $0.004 \text{ s}^{-1}$  from the slope of the curve. The different rate constants may be related to their different polarity and the degree of adsorption onto the surface of nanotubes.

To understand the high photocatalytic performance of the ZnO nanotubes, measurement of the optical properties was also performed. UV-vis diffuse reflectance spectrum of the nanotubes on an ITO glass substrate was used to determine the band gap (Figure 5), from which a band gap of  $3.13 \text{ eV}$  was obtained. This band gap is not only smaller than the well-known band gap of  $3.37 \text{ eV}$  for bulk ZnO but also slightly lower than that of the reported ZnO nanowires ( $3.22 \text{ eV}$ ).<sup>4,21</sup> The lower band gap makes it easier for the formation of photoinduced electrons and holes for ZnO nanotubes, which facilitates the electron transfer in the process of photodegradation of dye molecules. As a result, it can be concluded that the lower band gap of ZnO nanotubes in this work accounts for their enhanced photocatalytic activity. Recently, Kim *et al.* demonstrated that aqueous electrolytes could penetrate into a  $\text{TiO}_2$  nanotubular layer,<sup>22</sup> suggesting that similar wetting behavior of ZnO nanotubes is feasible and the large area-to-volume ratio of the ZnO nanotubes (both the inner and outside surface) may contribute to their high photocatalytic performance. More studies would be needed to understand the mechanism of photocatalytic activity of ZnO nanotubes.

The photocatalytic activities of ZnO nanotubes are further investigated and compared with other morphologies of ZnO nanostructure. ZnO thin films, ZnO nanowires, and ZnO nanotubes are prepared at the similar mass density of  $\sim 0.03 \text{ g/cm}^2$ , and their degradation  $\ln(C/C_0)$  using RB as test dye were plotted as a function of irradiation time, as shown in Figure 6. As summarized in the inset of Figure 6, the reaction constants for ZnO thin films, nanowires, and nanotubes were measured to be 0.007, 0.008, and 0.018, respectively. This comparison study reveals that the reaction constant by ZnO nanotubes is 157% larger than ZnO thin films. It is also 125% larger than ZnO nanowires, indicating that ZnO nanotubes showed enhanced photocatalytic activity compared with ZnO thin film or nanowires. The enhanced photocatalytic activity of ZnO nanotubes is mainly attributed to larger effective surface area, as can be suggested in SEM images of ZnO nanotubes, nanowires, and thin film (Figure 6b–d).

In summary, ZnO nanotubes were synthesized on flexible and glass substrates by using the Ga-catalyzed vapor phase

growth method. The low melting point of Ga enables us to synthesize the nanotubes at low temperature of  $80 \text{ }^\circ\text{C}$ . The nanotubes have also been demonstrated to serve as effective photocatalysts for the degradation of both RB and PAZO. Therefore, this work demonstrates a novel and simple way to synthesize ZnO nanotubes on flexible substrates using Ga as catalyst for low temperature growth. It can be expected that the low temperature growth process for ZnO nanotubes in this work could be attractive for the preparation of photocatalysts on flexible substrates, which possesses potential applications for the degradation of organic pollutants in water. The photocatalytic activity of ZnO nanotubes was shown to be much enhanced compared with ZnO thin films and ZnO nanowires, suggesting that the tubular structure of ZnO could be more effective photocatalysts compared with thin films or nanowires.

**Acknowledgment.** X. M. Zhang thanks the fellowship support by China Scholarship Council (CSC) (No. [2007] 3020). M. Wei thanks the Program for New Century Excellent Talents in University (Grant No.: NCET-05-121).

## References and Notes

- (1) Sun, Y.; Fuge, G. M.; Fox, N. A.; Riley, D. J.; Ashfold, M. N. R. *Adv. Mater.* **2005**, *17*, 2477.
- (2) Qin, Y.; Wang, X. D.; Wang, Z. L. *Nature* **2008**, *451*, 809.
- (3) Wang, X. D.; Song, J. H.; Liu, J.; Wang, Z. L. *Science* **2007**, *316*, 102.
- (4) Cun, W.; Wang, X. M.; Xu, B. Q.; Zhao, J. C.; Mai, B. X.; Peng, P.; Sheng, G. Y.; Fu, H. M. *J. Photochem. Photobiol. a-Chem.* **2004**, *168*, 47.
- (5) Yang, J. L.; An, S. J.; Park, W. I.; Yi, G. C.; Choi, W. *Adv. Mater.* **2004**, *16*, 1661.
- (6) Tian, Z. R. R.; Voigt, J. A.; Liu, J.; McKenzie, B.; McDermott, M. J.; Rodriguez, M. A.; Konishi, H.; Xu, H. F. *Nat. Mater.* **2003**, *2*, 821.
- (7) Kuo, T. J.; Lin, C. N.; Kuo, C. L.; Huang, M. H. *Chem. Mater.* **2007**, *19*, 5143.
- (8) Yao, Z.; Postma, H. W. C.; Balents, L.; Dekker, C. *Nature* **1999**, *402*, 273.
- (9) Cheung, C. L.; Hafner, J. H.; Lieber, C. M. *Proc. Natl. Acad. Sci. U.S.A.* **2000**, *97*, 3809.
- (10) Kim, P.; Lieber, C. M. *Science* **1999**, *286*, 2148.
- (11) Iijima, S. *Nature* **1991**, *354*, 56.
- (12) Goldberger, J.; He, R. R.; Zhang, Y. F.; Lee, S. W.; Yan, H. Q.; Choi, H. J.; Yang, P. D. *Nature* **2003**, *422*, 599.
- (13) Margulis, L.; Salitra, G.; Tenne, R.; Talianker, M. *Nature* **1993**, *365*, 113.
- (14) Zhang, M.; Bando, Y.; Wada, K. *J. Mater. Res.* **2001**, *16*, 1408.

- (15) Miyaji, F.; Davis, S. A.; Charmant, J. P. H.; Mann, S. *Chem. Mater.* **1999**, *11*, 3021.
- (16) Satishkumar, B. C.; Govindaraj, A.; Vogl, E. M.; Basumallick, L.; Rao, C. N. R. *J. Mater. Res.* **1997**, *12*, 604.
- (17) Xing, Y. J.; Xi, Z. H.; Zhang, X. D.; Song, J. H.; Wang, R. M.; Xu, J.; Xue, Z. Q.; Yu, D. P. *Solid State Commun.* **2004**, *129*, 671.
- (18) Hu, J. Q.; Bando, Y. *Appl. Phys. Lett.* **2003**, *82*, 1401.
- (19) Zhang, J.; Sun, L. D.; Liao, C. S.; Yan, C. H. *Chem. Commun.* **2002**, 262.
- (20) Wu, J. J.; Liu, S. C.; Wu, C. T.; Chen, K. H.; Chen, L. C. *Appl. Phys. Lett.* **2002**, *81*, 1312.
- (21) Wu, J. J.; Liu, S. C. *J. Phys. Chem. B* **2002**, *106*, 9546.
- (22) Kim, D.; Macak, J. M.; Schmidt-Stein, F.; Schmuki, P. *Nanotechnology* **2008**, *19*, 5.

JP901011U